

# Investigation of Air Gaps Entrapped in Protective Clothing Systems

Il Young Kim<sup>1,\*</sup>, Calvin Lee<sup>1</sup>, Peng Li<sup>2</sup>, Brian D. Corner<sup>1</sup> and Steven Paquette<sup>1</sup>

<sup>1</sup>US Army Soldier and Biological Chemical Command, Natick, MA 01760, USA

<sup>2</sup>GEO-CENTERS, Inc., Newton, MA 02459, USA

Air gaps entrapped in protective clothing are known as one of the major factors affecting heat transfer through multiple layers of flexible clothing fabrics. The identification and quantification of the air gaps are two aspects of a multidisciplinary research effort directed toward improving the flame/thermal protective performance of the clothing. Today's three-dimensional (3-D) whole body digitizers, which provide accurate representations of the surface of the human body, can be a novel means for visualizing and quantifying the air gaps between the wearer and his clothing. In this paper we discuss how images from a 3-D whole body digitizer are used to determine local and global distributions of air gaps and the quantification of air gap sizes in single and multilayer clothing systems dressed on a thermal manikin. Examples are given that show concordance between air gap distributions and burn patterns obtained from full-scale manikin fire tests. We finish with a discussion of the application of air gap information to bench-scale testing to improve the protective performance of current flame/thermal protective clothing. Copyright © 2002 John Wiley & Sons, Ltd.

## INTRODUCTION

A flame/thermal protective garment consisting of multiple layers of fabrics does not fit tightly on a complex human body surface. The clothing fabrics are more compressed in some areas than others. Air gaps usually exist between flexible fabric layers and on the body surface, especially in loose areas. When a soldier in protective clothing is exposed to a heat source, heat is transferred through this mixed medium of solid fabrics and gaseous air.

The mechanism of heat transfer through this medium is complex. It is likely that conduction takes place through the contact points of the fabric, while convection and radiation occur across the trapped inter-facial air.<sup>1</sup> Past experiments have demonstrated that the air gap size is critical: if the gap is too small, heat passes across the space easily; if the gap is too large, convection may begin, which reduces the effectiveness of the thermal barrier.<sup>2,3</sup> Even the thermal conductivity of a fabric is dependent on the amount of air trapped in it. While an increase in the volume of air will decrease thermal conductivity, it will also allow more incident radiation to penetrate through a fabric.<sup>4</sup> The volume of air per unit area provides a basis for estimating the thermal insulation of multiple layers of fabrics.<sup>5</sup> Quantifying the size and distribution of air gaps in thermal protective clothing as it is worn has been difficult. A limiting factor was the lack of an imaging technology that afforded a view of the air spaces between the skin and the fabric. Three-dimensional surface digitizing provides accurate surface models of skin and clothing layers that can be used to compute the amount and distribution of air trapped between the surfaces. The size and distribution of air gaps measured

will be examined based on the geometry of the human body. The burn injury data collected from full-scale fire tests will be compared with the air gap data to see how they relate to the location and percentage of burn injury.

## EXPERIMENTAL

### Materials (manikin and clothing systems)

For this study, a thermal manikin (40 regular male) was digitized in a number of clothing conditions using a whole body surface digitizing system (four camera) in the 3-D Anthropometry Laboratory at the U.S. Army Natick Soldier Center (Natick, MA). System resolution is so good that approximately 300 000 points (XYZ coordinates) comprise an image of an average sized person.<sup>6</sup> The thermal manikin, developed by DuPont, conforms to ASTM standard F1930-99. The manikin head and legs cannot move and the arms have limited rotation at the shoulders and hands. There are 124 25 mm diameter holes evenly distributed over the manikin for the thermal sensors.

Plate 1 shows the locations of the holes for skin sensors distributed around the thermal manikin. The holes are shown on the manikin picture on the left as the orange colored dots, and the numbered areas centred with the holes are shown in the illustrated drawings. For the scanning, the holes were covered with bright orange self-adhesive paper dots. The colored dots covered the holes that would otherwise register as voids, and provided a noticeable marker for later mapping in sensor locations. Three different colors are used to show the location of the sensors positioned at both sides of the

\*Correspondence to: Il Young Kim, US Army, SBCCOM, AMSSB-RIB-M, Kansa Street, Natick, MA 01760-5019, U.S.A.

head, torso, arms and legs. Pink is for the front or rear, blue is for the outer side and green is for the inner side (Plate 1). Each numbered area is the theoretical area covered by a sensor that is located in the middle of the area. For this study, the sensors were grouped in eight different areas as shown in Table 1. The torso area consists of chest and abdomen areas.

Table 2 shows the current military flame/thermal protective clothing ensembles for the army aviators and tankers in five configurations, each providing a different level of protection. The basic outfit is a coat and trousers for aviators, and a combat vehicle crewmen (CVC) coverall for tankers. Both are made of the same fabric of Nomex/Kevlar/P140 plain weave. Color is the only difference between them: a woodland camouflaged pattern for the coat and trousers, and olive green 106 for the CVC coverall. When the configuration number increases from 1 to 3, the underwear changes from T-shirt and briefs to cotton underwear, and to Nomex underwear while keeping the basic outfit. For configuration 4, a cold weather (CW) jacket is added, and for configuration 5 another bib overall is inserted. The

**Table 1. Sensors in eight different areas**

Areas	Front	Rear
Chest	61 62 63 64 65 66	92 96 97 98 99 100
	67 68 69 73 74 75	101 102 103 105
	76 77 93 94 95	107 108 109 111
Abdomen	70 71 72 78 79 80	110 112 113 114
	84 88 89 90 91	115 116 117 118
Left Leg	30 31 33 34 35 38	29 32 36 37 40 41
	39 42 43 85 86 87	44 119 121 122
Right Leg	46 47 49 50 51 54	45 48 52 53 56 57
	55 58 59 81 82 83	60 120 123 124

**Table 2. Ensemble items of five configurations of current military protective clothing (a: aviator, b: tanker)**

Configuration	Component protective clothing end items (thickness)
1	a Coat and trousers, aircrew + T shirt and Briefs (2.54 mm) b CVC coverall + T-shirt and briefs
2	a Coat and trousers, aircrew + cotton underwear (3.4 mm) b CVC coverall + cotton underwear
3	a Coat and trousers, aircrew + Nomex underwear (3.3 mm) b CVC coverall + Nomex underwear
4	a Jacket, CW, aircrew/liner + 3a (10.4 mm) b Jacket, CW, CVC + 3b
5	a Jacket, CW, aircrew/liner + bib overall + 3a (17.8 mm) b Jacket, CW, CVC + bib overall + 3b

ensembles for aviators (configuration 1a–5a) were chosen for this 3-D scanning investigation.

## Method

**3-D scanning.** Data collection began by scanning the nude manikin. The manikin was positioned within the scanning volume so as to maximize surface exposure. The arms were moved away from the body in separate scans to improve data capture along the torso and under the arms. In addition to vertex and mesh data, a color map was saved with the initial scan to locate the position of the heat sensors. This was done to better match our results with those from full-scale burn tests. Manikin preparation was the same for all clothing conditions. Potential void areas, such as the black and dark brown shades in the battle dress uniform (BDU) camouflage, were taped over with white cloth tape or dusted with cornstarch to improve reflectivity. Collars, pockets, buttons, seams and other attachments or findings were taped down with cloth tape. Just before scanning, the fabric was smoothed and checked for a natural drape.

**Measuring air gaps.** The method for measuring the air trapped between clothing and skin is based on the observation that when clothing is put on, the surface of the clothing is displaced away from the underlying surface. We assume that, after taking the thickness of the material into account, the displacement of the clothing surface is due to air trapped in the clothing layer.

The displacement of the new surface relative to the original surface is measured in the following manner. First a scan is made of the initial surface. In our case, the thermal manikin serves as the base surface. Next, the clothing is put on the manikin and a second scan is taken. The two scans are then superimposed using a region unchanged in both scans. Once the two scans are aligned, cross-sections of the scan pair are taken along their vertical axis. The cross-section displays two contours that alternately coincide or are separated by some distance. The distance between contour lines is the air gap.

The next step is to construct two vectors,  $D_1$  and  $D_2$ , that originate at the centroid of the initial scan cross-section and are oriented in the same direction. Vector  $D_1$  is drawn to the first contour while  $D_2$  is drawn to the second contour (Fig. 1).

Because vectors  $D_1$  and  $D_2$  share the same orientation, they differ in magnitude only. Subtracting  $D_1$  from  $D_2$  gives the distance between the scan pair surfaces at a given point along their contour lines. The term ' $D_2$  minus  $D_1$ ' is the difference vector.

If the difference vector is greater than the thickness of the clothing plus a small error term, then the distance represents an air gap. The set of all difference vectors between two surfaces is termed the distance field. Figure 1 illustrates how the difference vector is computed.

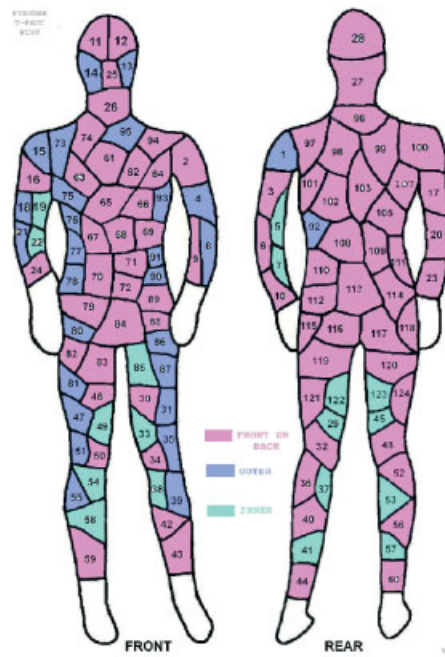
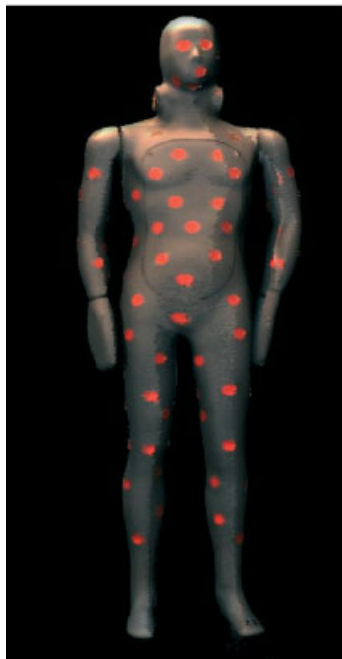
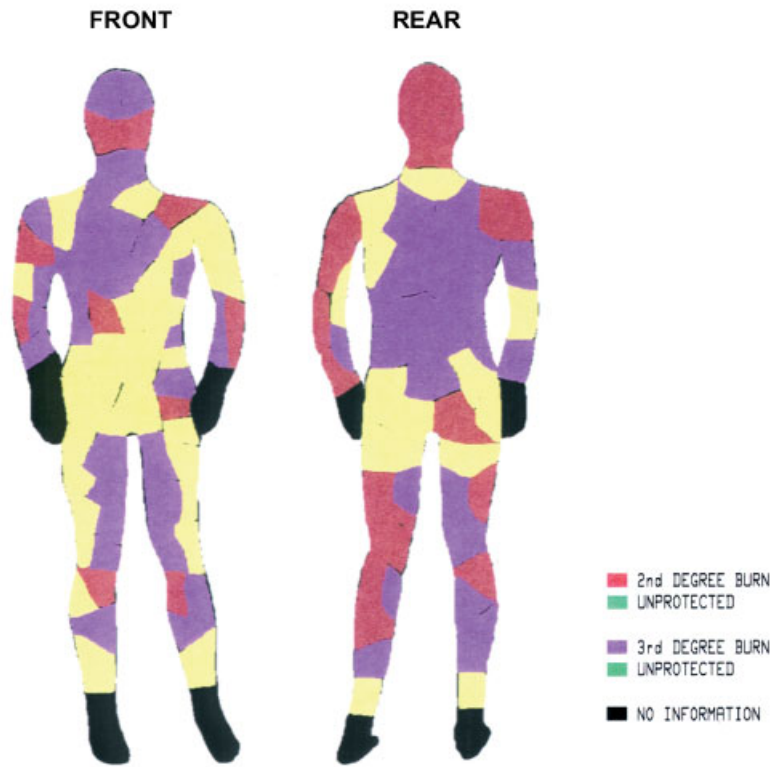
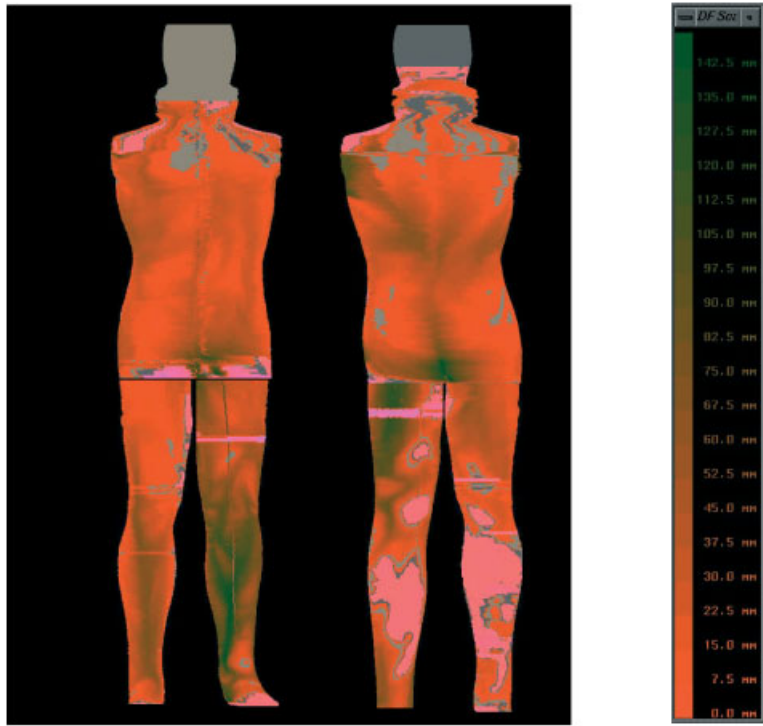
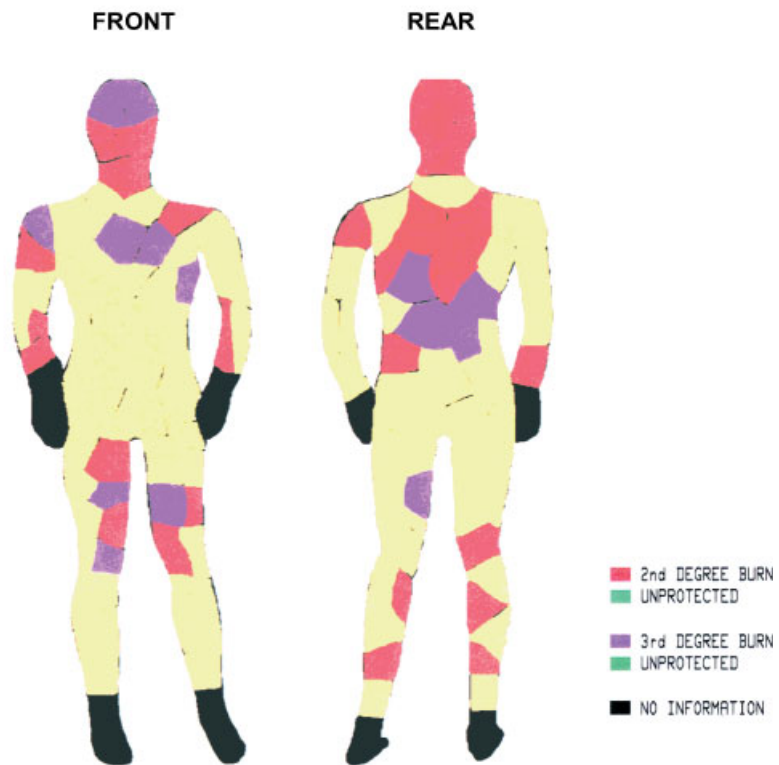
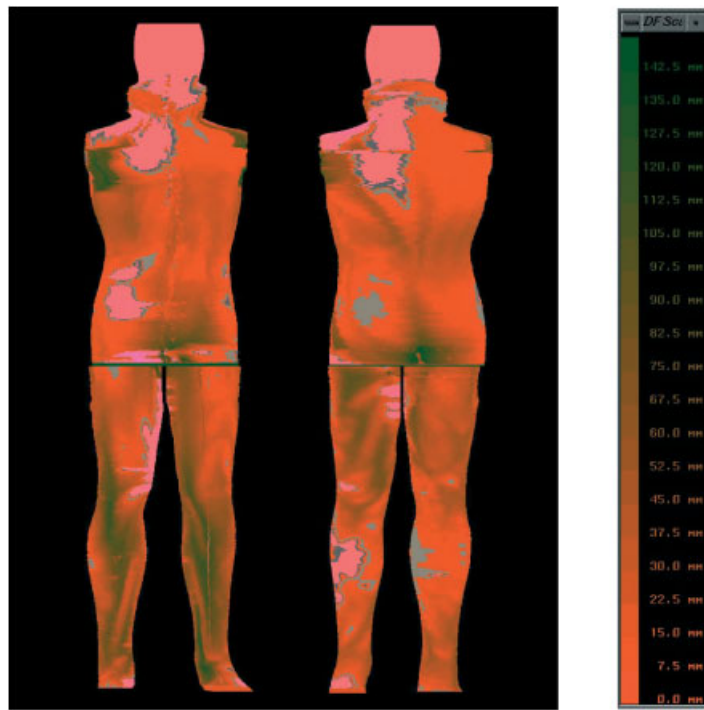


Plate 1. Sensor locations on a thermal manikin.



**Plate 2.** Air gap distribution image (top) compared with burn injury locations (bottom) for configuration 1 protective clothing ensemble (heat source:  $84 \text{ kW/m}^2$ , exposure time: 6 s).



**Plate 3.** Air gap distribution image (top) compared with burn injury locations (bottom) for configuration 3 protective clothing ensemble (heat source:  $84 \text{ kW/m}^2$ , exposure time: 6 s).

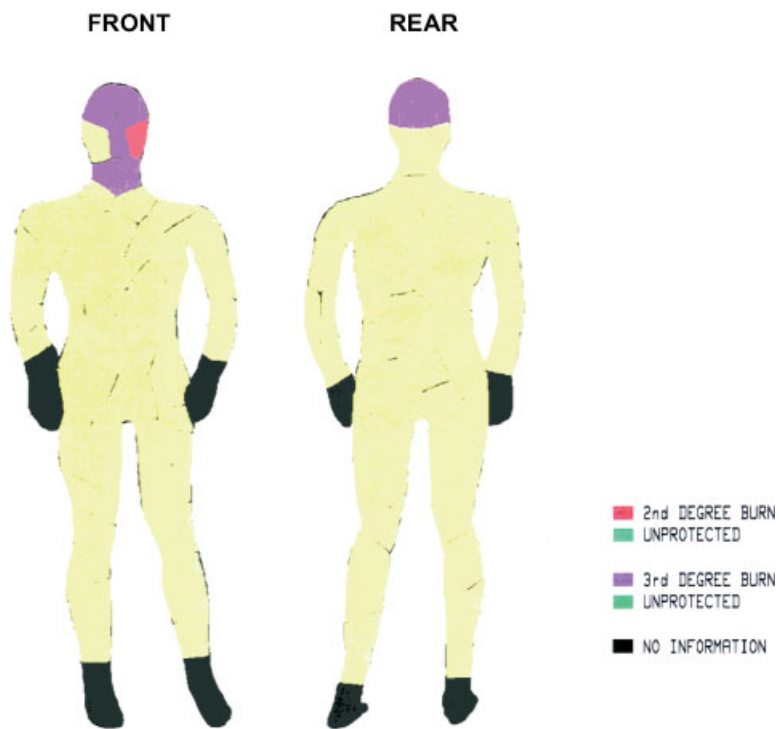
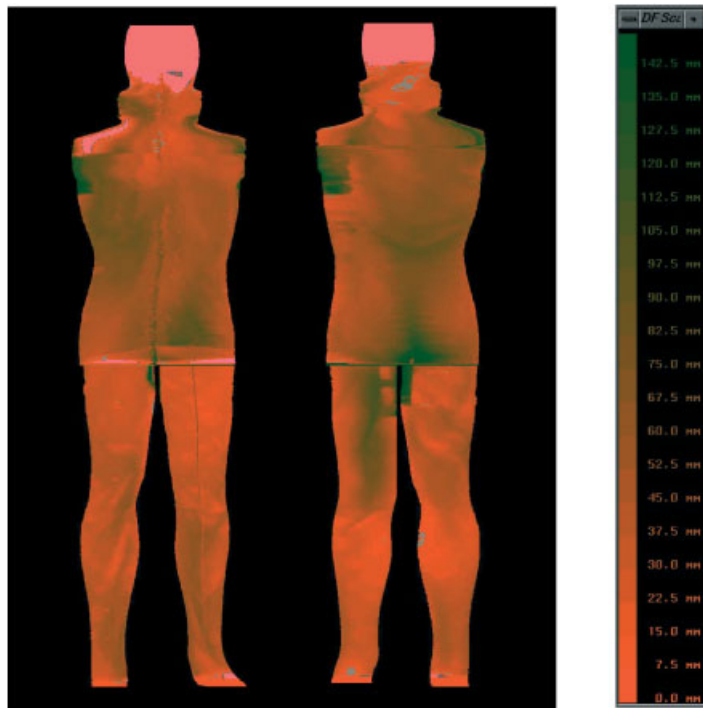


**Plate 4.** Air gap distribution image (top) compared with burn injury locations (bottom) for configuration 5 protective clothing ensemble (heat source: 84 kW/m<sup>2</sup>, exposure time: 6 s).

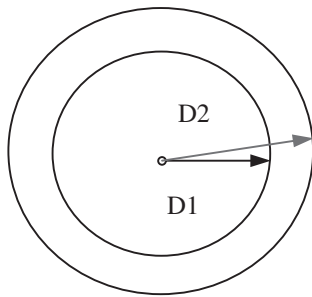


**Figure 1.** Illustration of how distance is computed between two superimposed surface scans.

## RESULTS AND DISCUSSION

Scans were taken of each clothing layer beginning with the nude manikin. With the exception of configuration 1, the manikin plus long underwear was defined as the base clothing condition for all comparisons.

Data were extracted from two scans: one with the arms rotated to a backward position (scan 1) exposing more of the front of the torso, and one with the arms rotated forward (scan 2) exposing more of the rear of the torso. The two scans were taken to improve visualization of the torso. Two changes were also made to the air gap data extraction process. First, air gaps were identified for the sensor locations only. Second, due to problems capturing the inside surface of the manikin arms, the arms were removed from the scans prior to data extraction.

The number of points per sensor area is dependent on the surface curvature and the void area. Most often the sample size was well over 100, and the points were distributed evenly across the sensor area. Average air gap values were relatively close in magnitude between scans 1 and 2, except for the values from sensors 75, 76 and 93. The large readings at those sensors were due to the inclusion of part of the upper arms in the distance vector calculation for scan 1 and can be ignored. The negative average air gap value at sensor 90 was from errors introduced with superimposition and void filling. Small negative values may be taken as zero. Larger negative values indicate a problem with alignment or void filling and require extra attention. The pattern of air gap distribution was quite consistent between scans. For the front of the manikin torso, the largest averages were found in the region below the chest level but above the pelvis (65, 66, 67, 60, 71, 72, 77, 78, 84, 89). The smallest average gaps, on the other hand, were located on the shoulders and chest (61, 62, 63, 64, 74, 95). Averages on the low side were also found in the buttock region (116, 117).

The number of successive clothing configurations add fabric layers for better protection. Configuration 1, consisting of two layers of fabric, provides the least protection while configuration 5, with eight layers of fabric, provides the most protection. Figure 2 shows the size and distribution of air gaps for four different protective clothing ensembles. The percentage of total number of sensors (%) on the figure shows the percent

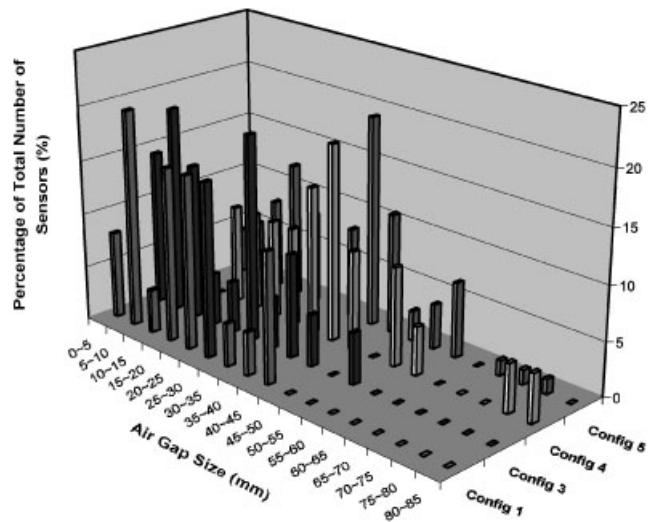


**Figure 2.** Air gap size and distribution for different configurations of protective clothing ensembles.

of the sensors for each configuration dispersed over 17 ranges of air gap size. The maximum size of air gap for configuration 1 was 45 mm. There was no big difference in air gap size between configurations 1 and 3. The only difference between them was underwear. A T-shirt/brief was used in configuration 1 and Nomex underwear in configuration 3. Nomex underwear is thicker, but more elastic than the T-shirt/brief combination. A jacket is added to configuration 3 to give configuration 4 and a bib overall is added to configuration 4 to complete configuration 5. The bib overall adds two more layers of fabric but it tightens all the inner garments so reducing the size of the air gaps within them. A maximum air gap of 85 mm was found in configuration 4. Not only the number of fabric layers but also the fabric characteristics such as flexibility and elasticity affect the number of air gaps entrapped among them.

The distribution of air gaps is likely to depend on the local geometry of the human body. Figure 3 shows air gaps entrapped in configuration 3 ensembles. There was some difference in the size and distribution of air gaps among four different human body areas. The size of most of the air gaps was below 30 mm (1.22 in), covering 82.35% of the whole body area: 20.25% of front torso and rear torso respectively, 27% of front legs and 14.85% of rear legs. It is interesting to note that both front and rear torsos showed exactly the same percentage, while the front legs showed the highest value and the rear legs the lowest. Air gaps below 10 mm (0.408 in) were distributed over 30.42% of the manikin: 9.45% of front torso, 10.8% of rear torso, 6.12% of front leg and 4.05% of rear legs. These are the areas susceptible to burn injury. Some exceptionally big air gaps observed in the rear torso and front legs areas could have been from wrinkles or folds in the garment.

There are 15 skin sensors distributed over the front chest area. Five of them, 61, 62, 63, 74 and 95, cover the upper chest area while another five, 75, 76, 77, 93 and 69, cover both the side areas, including the armpits. The geometry of the upper chest area is most likely to be convex and that of both side areas concave. Figure 4

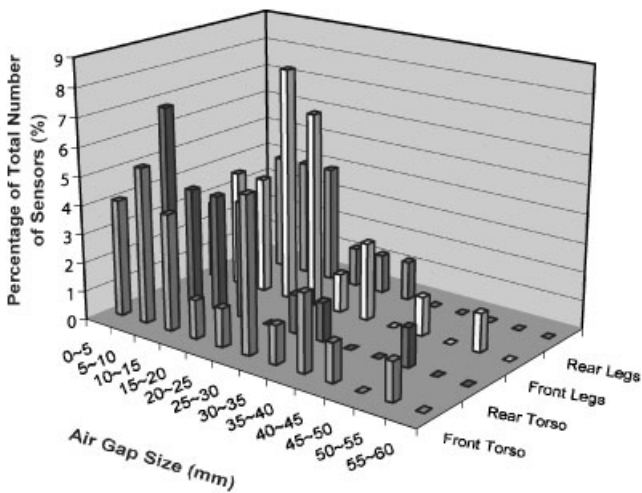


**Figure 3.** The size of air gaps distributed on four different areas (configuration 3).

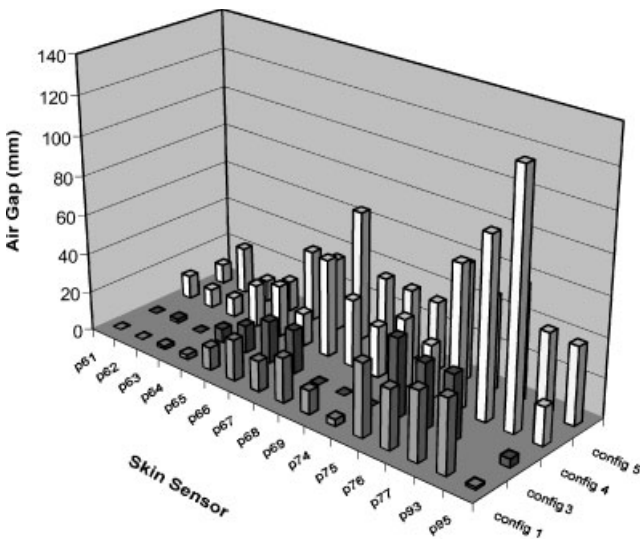


**Figure 4.** Air gap size at sensor locations for four different configurations (front chest area).

shows the difference in air gap size between these two areas. The sensors covering the convex area showed smaller air gaps than those covering the concave areas. It is not surprising that the smallest air gaps were found in other convex areas such as the shoulders and upper rear chest area (covered with skin sensors 97, 98, 99 and 100). The convexity of the human body surface is a major factor influencing the number of air gaps within any selected garment. This is a practical way to estimate the number of air gaps on a specific surface area.

Another way of assessing the distribution of air gaps over the manikin is to count the number skin sensors within a range of specific air gaps. Figure 5 shows the relationship between the number of sensors and the size of the air gap. The number of sensors recording below 1/2 in (12.7 mm) reached 48.71% for configuration 1 and 58.1% for configuration 3. Below 1/4 in (6.35 mm), the

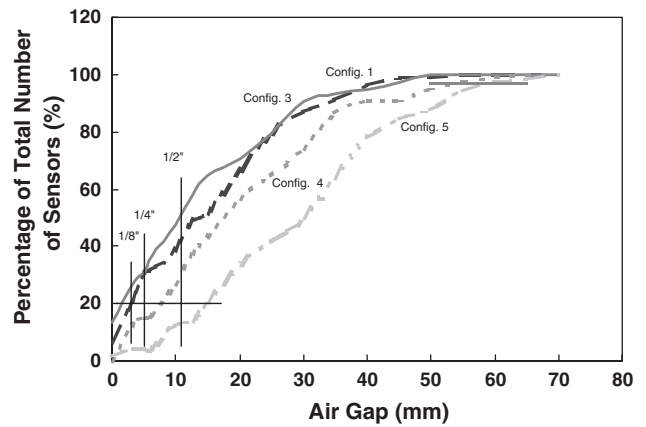


**Figure 5.** Distribution of air gaps based on their size levels.

distribution decreased to 32.05% and 36.48%, respectively. They showed the same 24% for < 5 mm air gap. Exactly 20% of the total sensors covering configuration 1 had air gaps below 1/8 in (3.17 mm). In the case of configuration 3, the same 20% of total sensors were below 1/16 in (1.58 mm) air gap. As seen on the graph, configuration 3 had more sensors than configuration 1 at most air gap sizes. This might be because the Nomex underwear of configuration 3 fits tighter on the surface of the manikin than does the T-shirt/briefs of configuration 1. Currently a burn injury below 20% of the whole body is one of the protective performance criteria for a military flame/thermal protective clothing system. A protective garment, causing more than 20% burn injury when exposed to a specific heat flux for a specific time, is not performing as required. This information is very useful when evaluating whether flame-retardant fabrics meet the requirement using a bench-scale test apparatus. The sizes of the air gaps covering 20% of the whole body can be set on a bench-scale testing.

The distribution of air gaps around the surface of the manikin is shown with a color code (Plates 2–4). In the code, a brighter color indicates a smaller size of air gap. This image shows the exact locations and sizes of air gap expressed with a different color on the manikin. To check the reproducibility of these data, the same garment was dressed on the manikin three times. The difference in the results was negligible. The air gap images provide no information for the head and arms as these are not available from 3-D images. The dots in gray on the images represent negative distances that mean realistically no air gaps at all. The darker (greener) the color, the bigger the air gaps are. The advantage of this image is that the air gap data can be compared with burn injury data from the PyroMan full-scale test done at the North Carolina State University.<sup>4</sup> For the testing, the same manikin was dressed with the same configuration ensemble and then exposed to a heat flux of 84 Kw/m<sup>2</sup> for 6 s. Eight propane torches were aimed at the manikin in four directions and two levels for each direction. Plates 2–4 show comparisons between them for three different configurations; Plate 2 is for configuration 1 with the lowest protection level, Plate 3 for configuration 3, and Plate 4 for configuration 5 with the

most protection. The comparison serves to correlate the location of burn injury with the size of air gap for the same configurations. The areas with fewer air gaps are shown to be more susceptible to burn injury. Although they do not agree in exact locations, they agree in general burn injury pattern and total percent of burn injury.

For configuration 1, the full-scale test showed a total of 65% burn injury, 22% of 2nd degree burn and 43% of 3rd degree burn. Configuration 3 showed much less burn injury with a total of 33% burn injury, 22% of 2nd degree burns and 11% of 3rd degree burn. Configuration 5 showed almost no burn injury, only 2% of 3rd degree burns on the head area.<sup>7</sup>

The color-coded images show how air gaps of different sizes were distributed around the surface of the manikin. It is easily observed that some areas had more air gaps entrapped than other areas and some air gaps were bigger than others. One of the factors controlling the number of air gaps is the convexity of the human body surface and the location of garment gravity resting on it. Generally, more air gaps exist in concave areas; whereas, smaller air gaps exist in convex areas. Almost no air gaps were observed in such convex areas as the shoulder and upper chest areas where the gravity of the garment is resting. The images show that the smallest air gaps were in the shoulders and rear upper chest areas while the biggest air gaps were in the side torso areas. The trousers are designed to be hung around the legs and do not fit leg surfaces as tightly as the jacket. This is why the distribution of air gaps around the legs is affected by the temporary position of the trouser fabric, which tends to be transitory, rather than the geometry of the legs.

Of course, air gaps are just one of several factors affecting the severity of burn injury. Another factor is the flame retardancy of the selected protective clothing fabric. For example, more air gaps can be entrapped within loose T-shirts and briefs (configuration 1) than within elastic Nomex underwear (configuration 3) that fits tightly. However, Nomex underwear is flame retardant while T-shirts and briefs are not. This is why configuration 3 with fewer air gaps shows less burn injury than configuration 1.

---

## CONCLUSIONS AND FUTURE WORK

---

Some anecdotal evidence from the medical literature and limited visual comparison with full-scale burn tests have indicated that the air gap distribution matches the pattern of burn severity. That is, burn severity increases as the air gap decreases. Data from bench-scale testing showed that a fabric sample with a 1/4 in air gap caused no burn injury while the same sample without an air gap caused 2nd degree burn injury<sup>8</sup> 7.7 s after exposure to a heat flux of 84 kW/m<sup>2</sup>. Convection may indeed occur within larger air spaces, however, the trapped air seems to provide an insulation layer. As a whole, the result of this study agrees with the theory.

It had been thought that the size and distribution of air gaps entrapped in a garment was randomly dispersed

or at least unpredictable. This study, however, has discovered that the size and distribution of air gaps depend on the drape of the protective garment fabrics as they rest on the underlying geometry of the human body surface. Based on this information, it is quite possible to estimate the location, as well as the severity, of burn injury for selected protective ensembles. Generally, the shape of all male human bodies is alike even though their sizes are different. So, this kind of information is applicable to most protective garments for both military and civilian personnel.

This is the first time that air gap distance has been calculated for clothing items as they are worn. Data extracted for the military flame/thermal protective clothing demonstrate that 3-D whole body digitizing provides a unique view into the size and distribution of air gaps in a common clothing ensemble worn by U.S. Army soldiers.

Our goal in this research was to provide a structure for the integration of bench tests and full-scale burn tests so that predictions from one set of experiments can be applied more readily to the other method of investigation. Quantifying air gaps in clothing as it is worn provides information that spans the two test strategies. We have completed an initial investigation of air gap size and distribution of clothing worn by U.S. Army aviators. We will continue our study with an analysis of protective clothing worn by tank crew members.

During the next phase of study we will be refining our data extraction algorithms to match better thermal sensor data from full-scale burn tests. Mapping the data on the manikin will allow us to visualize heat transfer across known air gaps. More details of local comparisons of burn injury between bench scale and full scale will be included in another paper that will be published later.

We will improve our post-processing functions to better handle slight misalignments, and to fill voids on curved surfaces more precisely; thereby eliminating the negative distance values. We will also investigate ways of quantifying air trapped between the middle layer of a three-layer ensemble. This will require an analysis of clothing compression so that we can predict when an initial air gap may fall to zero after being covered by a layer of clothing.

For this study, the size of the air gap is assumed to remain constant throughout the exposure. In practice, the amount of air gap will keep changing as long as a soldier dressed in the clothing moves around. A soldier escaping from battlefield fire hazards will show several different movements of the human body. Therefore, a variety of postures such as bending, running, or crouching, will also be investigated with this scanning. This study will be extended to a female manikin that is expected to provide a slightly different result because of the different geometry of the body surface.

## Acknowledgements

The author of this paper greatly appreciate the contribution of the Center for Research on Textile Protection and Comfort, College of Textiles, North Carolina State University to this work.

## REFERENCES

- 
1. Kreith F. *Principles of Heat Transfer*. International Textbook Company; Scranton, 1960.
  2. Torvi DA, Dale JD, Falkner B. *J. Fire Prot. Engr.* 1999; **10**: 1–12.
  3. Chianta MA, Stoll AM. *Aerospace Med.* 1964; **40**: 1232–1238.
  4. Torvi DA, Dale JD, Falkner B. *Textile Res. J.* 1998; **68**: 787–796.
  5. Morris MA. *Textile Res. J.* 1955; 766–773.
  6. Li P, Corner BD, Paquette S, Lee C, Kim IY. *Proceedings of The Human Factors and Ergonomics Society Conference, 30 July–4 August, 2000; San Diego, California.*
  7. *A Report on the Thermal Protective Performance (TPP) and the PyroMan Evaluation*. Center for Research on Textile Protection and Comfort, College of Textiles, North Carolina State University, 1999.
  8. Wu PK. Factory Mutual Research Corporation; Technical Report, J.I.0003008964, 2000.